CME LIVE OPEN ACCESS

Vaccine and Immunization-Research and Development

Mini Review Article

Brain and Eye Coordination in Alzheimer's disease

Kunal Joon*

University of Noida International Institute of Medical Sciences.

Corresponding Author: Kunal Joon, University of Noida International Institute of Medical Sciences.

Received: 2024 Feb 19 **Accepted:** 2024 Mar 10 **Published:** 2024 Mar 20

Abstract

The eye is the anatomical extension of brain where multiple parallels can be drawn between the neurons, vasculature and immune response. Further both organs modify similar with diseases. As such stands to reason that multidisciplinary research that investigates neurodegenerative diseases.

Keywords: Neurodegenerative Diseases, Alzheimer's Disease, Vascular Diseases Parkinson's Disease, Dementia, Optic Nerve, Neuroimaging, Subcortical Infract, Optical Coherence Tomography And Macula.

Alzheimer's disease

Most common form of dementia. Alzheimer's disease is associated with hall mark, amyloid beta in the retina [1]. As shown in the diagnosis in the following

Table 1 AD, Alzheimer's disease; DLB, dementia with Lewy bodies; CVD, Cerebrovascular dementia; FTLD-TDP, frontotemporal lobar degeneration with TDP-43 inclusion; CAA cerebral amyloid angiopathy; HS, Huntinaton's disease; N/A, not applicable (Control eves).

Case no	Age	Sex	Primary Path DX	Additional Path DX	A- Beta(Thal, Biel) (1-5)	Braak Stage (1-6)	Neuritic Plaque (CERAD, Biel)	Diffuse Plaque (CERAD, Biel)
1	75	M	N/A	-	-	-	-	-
2	70	M	N/A	-	-	-	-	-
3	75	M	N/A	-	-	-	-	-
4	73	M	N/A	-	-	-	-	-
5	75	M	N/A	-	-	-	-	-
6	66	M	N/A	-	-	-	-	-
7	69	M	N/A	-	-	-	-	-
8	69	M	N/A	-	-	-	-	-
9	55	F	N/A	-	-	-	-	-
10	63	F	N/A	-	-	-	-	-
11	78	F	AD	-	5	6	Frequent	Frequent
12	88	F	AD	FTLD-TDP, CAA	5	6	Frequent	Frequent
13	59	F	AD	DLB	5	6	Frequent	Frequent
14	70	M	AD	CAA	5	6	Moderate	Frequent
15	80	M	DLB	mod, AD	3	4	Moderate	Frequent
16	94	F	AD	CAA	5	6	Frequent	Frequent
17	75	M	AD	DLB, CAA	5	6	Frequent	Sparse
18	82	F	AD	DLB	5	6	Frequent	Frequent
19	82	M	DLB	mod, AD	5	5	Moderate	Frequent
20	79	M	AD	_	5	6	Frequent	Frequent
21	87	F	CVD	mod, AD	5	4	Moderate	Frequent
22	82	F	AD	CAA	5	6	Frequent	Frequent
23	81	F	AD	mild DLB	5	6	Frequent	Frequent
24	89	F	CVD	mod, AD, FTLD-TDP	5	5	Moderate	Frequent
25	82	F	AD	HS, CAA	5	6	Frequent	Frequent

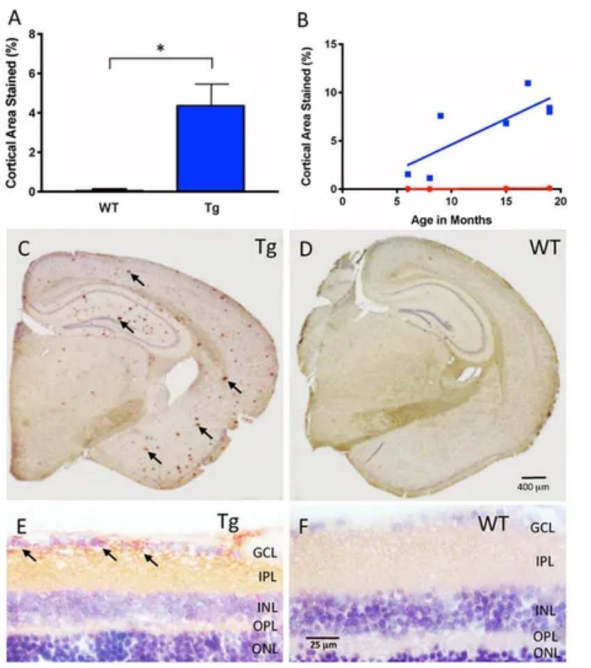

Figure 1: Immunohistochemical cortical 6E10 immunostaining. (A) Tg mice (blue) had significantly higher percentage of cortical area immunostained relative to their WT controls (red) (TG: 4.44% ± 1.50, N = 7; WT: 0.15% ± 0.08, N = 4; $p < 0.05$; Two-tailed Mann Whitney U test) [2]. (B) There was a trend towards higher cortical immunostaining in TG mice (blue) that begins at nine months of age. There was a moderately strong correlation and increase of immunostaining over time for TG mice ($r2 = 0.639$, slope = 0.53 ± 0.18, but not WT mice $r2 = 0.85$, slope = 0.006 ± 0.002; $p = 0.77$) [3]. (C) Representative cross-section of an 18 month TG mouse brain immunoreacted for Aβ. Note the numerous Aβ plaques shown by the red (AEC) chromogenic reaction product in cortex and hippocampal areas (arrows), compared to (D), the age-matched WT brain immunoreacted for Aβ. Scale bar for (C, D) is shown in D = 400 microns. (E) Retinal cross-section of an 18 month Tg mouse eye demonstrating Aβ immunoreactivity (arrows) in the inner retina in the ganglion cell layer (GCL) and the inner plexiform layer (IPL) compared to (F) the age-matched WT retina, which demonstrates a pale pink baseline level of immunoreactivity. Scale bar in D = 400 microns. Scale bar for (E, F) is shown in F = 25 microns denotes significance [4].

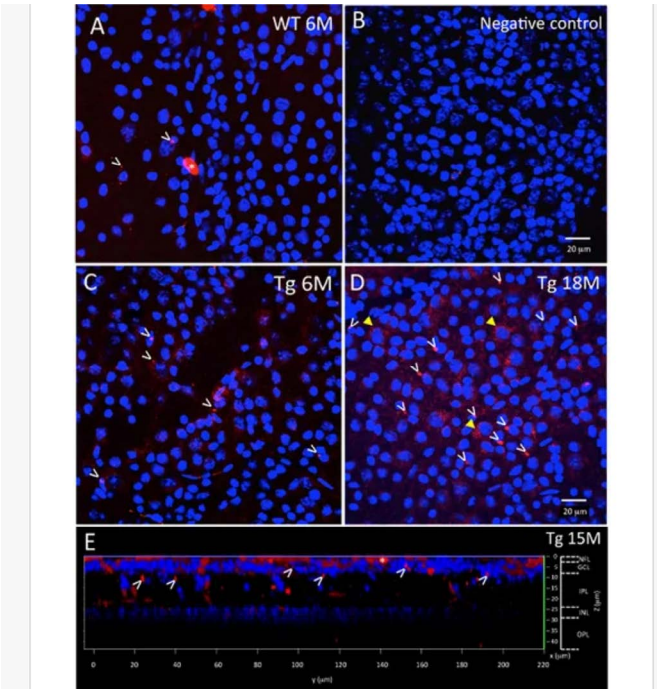

Figure 2: Also Shown In the Retinal Flurosence
Ex vivo WT and TG mouse whole mount and 6E10 immunofluroscence. Also shows (A) Representative confocal image after Aβ immunofluorescence of a younger (6 month) WT retina. Note the small specks of Aβ deposits in red immunofluorescence, some shown by white arrowheads. A larger opaque red profile is an artifact (white asterisk). (B) Representative image of a negative control section, in which the primary antibody was replaced with a non-specific IgG. Image demonstrates very low background levels of red immunofluorescence. (C) Representative image of Aβ immunoreactivity in the 6 month TG retina with representative red specks of immunofluorescence shown by white arrowheads [5]. (D) In an older (18 month) TG retina, the retinal immunofluorescence increased with more red immunoreactive specks (white arrowheads) and an occasional immunoreactive retinal ganglion cell (yellow arrowhead). (A–D) Scale bar: 20 µm. (E) An orthogonal view of the confocal z-stack reconstruction from a 15 month TG retina demonstrates that the majority of the Aβ immunoreactivity is present in the inner retina, specifically in the NFL and GCL. Some Aβ immunoreactive specks can be seen extending deeper into the IPL. Cell nuclear labeling with DAPI (blue) reveals lamination in the retina. Lamination and scale bars are shown on the right axes [6].

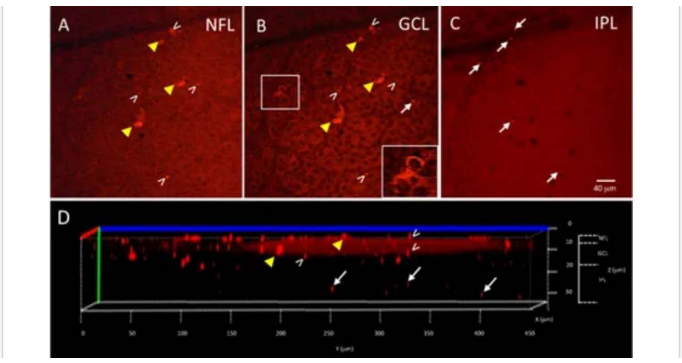

Figure 3: Also immmunofluroscence.

Representation of (A) Representative high power confocal image of the NFL demonstrating red immunofluorescence [7]. Note that Aβ specks can be seen in the NFL (white arrowheads), while the fluorescence associated with the RGC cell bodies in the GCL is also seen (yellow arrowheads). (B) As the confocal imaging descends into the wholemount, the GCL is identified in an optical slice by the presence of nuclei, here shown as black circular profiles as the DAPI channel is not shown. Note the fluorescence of the RGCs (yellow arrowheads) is evident in the cytoplasm (shown in boxed inset), and align with the RGCs seen in A. The extracellular Aβ specks can be seen (white arrowheads). (C) An optical slice through the IPL reveals fewer nuclei, as evidence by the lack of black circular nuclear profiles as seen in B. A few Aβ specks (white arrowheads) are seen, but generally less Aβ immunoreactivity is observed in IPL. Scale bar for (A–C) is shown in C = 40 microns. (D) The orthogonal view of the confocal z-stack reconstruction from the TG retina shown in (A–C). Note red immunoreactivity in the NFL, GCL and IPL (white arrowheads). The immunoreactivity present in the IPL (white arrows) indicates that the antibody penetrated deep into the wholemount tissue [8]. Additional optical slices from this wholemount are shown in

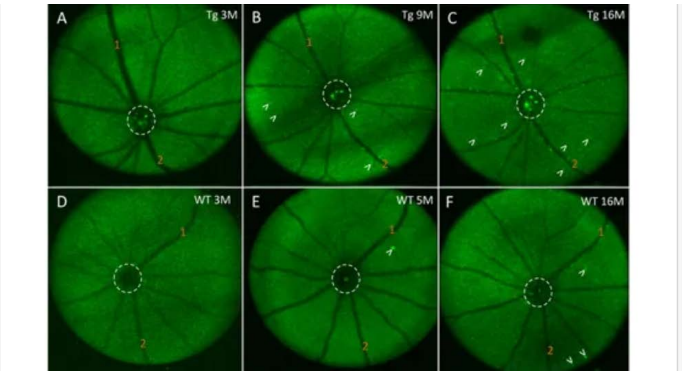

Figure 4: Also Flurosence of Mouse Retina.

In vivo fluorescence of the mouse retina after curcumin tail vein injections. (A–C) In vivo longitudinal fluorescence images of an individual TG mouse at 3, 9, and 16 months of age. (D–F) In vivo longitudinal fluorescence images of an individual WT mouse at 3, 5, and 16 months of age [9]. The pattern of Aβ in vivo fluorescence is seen as bright green specks (white arrowheads). Note that the Aβ in vivo fluorescent deposits increased as the animal aged. Representative landmark blood vessels are labeled with orange numbers and can be identified in each of the images in the TG (A–C) and in the WT (D–F). Dashed white circle indicates area of the optic nerve head. Representative examples of the in vivo longitudinal fluorescence images of an individual WT mouse at 3, 5, and 16 months of age reveals that Aβ fluorescent deposits only marginally increased as the animal aged (D–F). Note a significantly higher load of Aβ fluorescent deposits in the 16 month Tg (C) compared to the 16 month WT (F) mice [10].

Statistics

It indicates a two tailed Mann- Whitney U test, a two way ANOVA multiple comparison test with post hoc bonferroni.

Results

- Cortical Abeta Immunoreactivity is greater in TG than WT
- Retinal Abeta Immunoreactivity is greater in TG than WT

Treatment

Stem cell therapy or monoclonal genetic antibodies with required gene can help with condition also alizehmers treatment through gene therapy or stem cell therapy can lead to its treatment.

Discussion

- Brain eye coordination
- Alzheimer's disease
- Effect of eye during Alzheimer's disease

Conclusion

Brain eye coordination and effect of eye during Alzheimer's disease.

References

1. Bulovaite, E., Qiu, Z., Kratschke, M., Zgraj, A., Fricker, D. G., et al (2022). A brain atlas of synapse protein lifetime across the mouse lifespan. Neuron, 110(24), 4057-4073.
2. Bateman, R. J., Xiong, C., Benzinger, T. L., Fagan, A. M., Goate, A., et al (2012). Clinical and biomarker changes in dominantly inherited Alzheimer's disease. New England Journal of Medicine, 367(9), 795-804.
3. FLEX–Deals, C. N. C. Get Price Alerts.
4. https://scholar.google.com/scholar_lookup?&title=Evaluation+of+the+chorioretinal+thickness+changes+in+Alzheimer%E2%80%99s+disease+using+spectral-domain+optical+coherence+tomography%2E&journal=Clin%2E+Exp%2E+Ophthalmol%2E&author=Bayhan+H.+A.&author=Aslan+Bayhan+S.&author=Celikbilek+A.&author=Tanik+N.&author=G%C3%BCrdal+C.&publication_year=2015&volume=43&pages=145%E2%80%93151
5. https://scholar.google.com/scholar_lookup?&title=Amyloid+precursor+protein+%28APP%29+and+beta+A4+amyloid+in+the+etiology+of+Alzheimer%E2%80%99s+disease%3A+precursor-product+relationships+in+the+derangement+of+neuronal+function%2E&journal=Brain+Pathol%2E&author=Beyreuther+K.&author=Mas-

ters+C.+L.&publication_year=1991&volume=1&pages=241%E2%80%93251
6. Brookmeyer, R., Johnson, E., Ziegler-Graham, K., & Arrighi, H. M. (2007). Forecasting the global burden of Alzheimer's disease. Alzheimer's & dementia, 3(3), 186-191.
7. https://scholar.google.com/scholar_lookup?&title=-Pathophysiological+roles+of+amyloidogenic+carboxy-terminal+fragments+of+the+%CE%B2-amyloid+precursor+protein+in+Alzheimer%E2%80%99s-+disease%2E&journal=J%2E+Pharmacol%2E+Sci%2E&author=Chang+K.+A.&author=-Suh+Y.+H.&publication_year=2005&volume=97&pages=461%E2%80%93471
8. https://scholar.google.com/scholar_lookup?&title=Alzheimer%E2%80%99s+disease+in+the+human+eye%2E+Clinical+tests+that+identify+ocular+and+visual+information+processing+deficit+as+biomarkers%2E&journal=Alzheimer%E2%80%99s+Dementia&author=Chang+L.+Y.+L.&author=Lowe+J.&author=Ardiles+A.&author=Lim+J.&author=Grey+A.+C.&-author=Robertson+K.&publication_year=2014&volume=10&pages=251%E2%80%93261
9. Chen, G., Chen, K. S., Knox, J., Inglis, J., Bernard, A., et al (2000). A learning deficit related to age and β-amyloid plaques in a mouse model of Alzheimer's disease. Nature, 408(6815), 975-979.
10. Sidiqi, A., Wahl, D., Ma, D., Cui, J., Beg, M. F., et al (2020). In vivo retinal fluorescence imaging with curcumin in an Alzheimer mouse model. Frontiers in Neuroscience, 14, 556271.